HHS Public Access

Author manuscript

Acta Biomater. Author manuscript; available in PMC 2015 December 01.

Published in final edited form as:

Acta Biomater. 2014 December ; 10(12): 5128–5138. doi:10.1016/j.actbio.2014.08.016.

Effect of *NELL1* gene overexpression in iPSC-MSCs seeded on calcium phosphate cement

Jun Liu[1,2], **Wenchuan Chen**[1,2], **Zhihe Zhao**[1], and **Hockin H. K. Xu**[2,3,4,5]

[1]State Key Laboratory of Oral Diseases, West China Hospital of Stomatology Sichuan University, Chengdu 610041, China

[2]Biomaterials & Tissue Engineering Division, Dept. of Endodontics, Prosthodontics and Operative Dentistry, University of Maryland Dental School, Baltimore, MD 21201, USA

[3]Center for Stem Cell Biology & Regenerative Medicine, University of Maryland School of Medicine, Baltimore, MD 21201, USA

[4]Marlene and Stewart Greenebaum Cancer Center, University of Maryland School of Medicine, Baltimore, MD 21201, USA

[5]Department of Mechanical Engineering, University of Maryland, Baltimore County, MD 21250, USA

Abstract

Human induced pluripotent stem cell-derived mesenchymal stem cells (iPSC-MSCs) are a promising source of patient-specific stem cells with great regenerative potential. There has been no report on *NEL-like protein 1* (*NELL1*) gene modification of iPSC-MSCs. The objectives of this study were to genetically modify iPSC-MSCs with NELL1 overexpression for bone tissue engineering, and investigate the osteogenic differentiation of *NELL1* gene-modified iPSC-MSCs seeded on Arg-Gly-Asp (RGD)-grafted calcium phosphate cement (CPC) scaffold. Cells were transduced with *red fluorescence protein* (RFP-iPSC-MSCs) or *NELL1* (NELL1-iPSC-MSCs) by a lentiviral vector. Cell proliferation on RGD-grafted CPC scaffold, osteogenic differentiation and bone mineral synthesis were evaluated. RFP-iPSC-MSCs stably expressed high levels of RFP. Both the *NELL1* gene and NELL1 protein levels were confirmed higher in NELL1-iPSC-MSCs than in RFP-iPSC-MSCs using RT-PCR and Western blot ($p < 0.05$). Alkaline phosphatase (ALP) activity was increased by 130% by NELL1 overexpression at 14 d ($p < 0.05$), indicating that NELL1 promoted iPSC-MSC osteogenic differentiation. When seeded on RGD-grafted CPC, NELL1-iPSC-MSCs attached and expanded similarly well to RFP-iPSC-MSCs. At 14 d, *runt-related transcription factor 2* (*RUNX2*) gene level of NELL1-iPSC-MSCs was 2.0-fold that of RFP-iPSC-MSCs. *Osteocalcin* (*OC*) level of NELL1-iPSC-MSCs was 3.1-fold that of RFP-iPSC-MSCs ($p < 0.05$). *Collagen type I alpha 1* (*COL1A1*) gene level of NELL1-iPSC-MSCs was 1.7-

Correspondence: Dr. Hockin H. K. Xu, Professor, Biomaterials & Tissue Engineering Division, Department of Endodontics, University of Maryland Dental School, Baltimore, MD 21201 (hxu@umaryland.edu).

fold that of RFP-iPSC-MSCs at 7 d ($p < 0.05$). Mineral synthesis was increased by 81% in NELL1-iPSC-MSCs at 21 d. In conclusion, NELL1 overexpression greatly enhanced the osteogenic differentiation and mineral synthesis of iPSC-MSCs on RGD-grafted CPC scaffold for the first time. The novel NELL1-iPSC-MSC seeded RGD-CPC construct is promising to enhance bone engineering.

Keywords

calcium phosphate cement scaffold; gene therapy; induced pluripotent stem cells (iPSCs); *NELL1*; osteogenic differentiation

1. Introduction

The treatment of large bone defects caused by trauma, tumor resection or disease remains a significant clinical problem. Autologous bone grafting, as the current gold-standard, has disadvantages such as a limited amount of harvested bone and donor site morbidity. Alternative methods, such as allografts and xenografts, have disadvantages including potential immunogenicity and pathogen transmission. Bone tissue engineering, based on stem cells or osteoprogenitor cells combined with osteoconductive scaffolds, has emerged as an attractive alternative to meet the clinical needs in bone regeneration [1,2]. Recently, human induced pluripotent stem cells (iPSCs) generated by enforced expression of defined sets of transcription factors in somatic cells were used as a novel promising source of progenitor cells [3,4]. Patient-specific iPSCs can be derived from somatic cells with the potential to differentiate into cells of all three germ layers. In order to reduce the risk of tumorigenesis of pluripotent stem cells, mesenchymal stem cells (MSCs) were derived from iPSCs (referred to as iPSC-MSCs). They were demonstrated to possess great proliferative potential and were promising for regeneration medicine applications [5–7].

To date, only a few studies have investigated iPSC-MSCs for bone engineering [6,8]. iPSC-MSCs exhibited the ability to differentiate into the osteogenic lineage [9]. Villa-Diaz *et al*. further verified the capability of human iPSC-MSCs to regenerate bone *in vivo* [8]. iPSC-MSCs were induced to osteogenic lineage for 4 days and then transplanted into calvaria defects of immuncompromised mice for 8 weeks [8]. Micro-CT and histological analyses indicated *de novo* bone formation in the defects and confirmed the contribution of the transplanted iPSC-MSCs in the new formed bone. More recently, dense bone-like tissue matrix was formed by culturing iPSC-MSCs in perfusion bioreactors on decellularized bone cylinders [6]. The phenotypic stability of engineered bone constructs was confirmed after 12 weeks of subcutaneous implantation in immunodeficient mice [6].

Bone morphogenetic proteins (BMPs), powerful osteogenic growth factors, have been widely used to promote osteogenic differentiation and improve bone formation. In a recent investigation, iPSC-MSCs were genetically modified to overexpress BMP2 [10]. The *BMP2* gene-modified iPSC-MSCs enhanced osteogenic differentiation and bone mineral production, compared to iPSC-MSCs without gene modification [10]. Besides BMPs, NEL-like protein 1 (NELL1) is another key osteoinductive growth factor to promote bone regeneration [11–14]. Compared to BMPs which participate in multiple developmental

processes during embryogenesis, NELL1 is highly specific to the osteochondral lineage with less adverse effects, such as ectopic bone formation [12,15]. An investigation compared the effects of BMP2 and NELL1 on bone regeneration using bone marrow MSCs (BMSCs) transduced with *BMP2* gene or *NELL1* gene, respectively [11]. The histologic analyses showed that the BMP2-induced bone tissues were mainly filled with fatty marrow. In contrast, the NELL1-induced bone tissues were similar to new trabecular bone mixed with chondroid bone-like areas [11]. These results suggest that NELL1 may be promising for bone tissue engineering. To date, there has been no report on *NELL1* gene modification of iPSC-MSCs for bone tissue engineering.

Calcium phosphate biomaterials are an important for bone regeneration due to their similarity to bone matrix minerals [16–18]. Among them, calcium phosphate cements possess excellent biocompatibility, injectability, osteoconductivity and can be replaced by new bone [19–22]. One such cement is comprised of tetracalcium phosphate (TTCP) and dicalcium phosphate anhydrous (DCPA) and referred to as CPC [23–25]. Recently, CPC biofunctionalized with Arg-Gly-Asp (RGD) was demonstrated to be advantageous for enhancing cell attachment, proliferation, and osteogenic differentiation [10,26,27]. Both iPSC-MSCs and *BMP2* gene-modified iPSC-MSCs seeded on RGD-grafted CPC successfully underwent osteogenic differentiation [10]. However, *NELL1* gene modification of iPSC-MSCs and their behavior on CPC scaffold have not been reported.

The objectives of the present study were to genetically modify human iPSC-MSCs for NELL1 overexpression, and investigate the osteogenic differentiation of *NELL1* gene-modified iPSC-MSCs seeded on RGD-grafted CPC scaffold for the first time. The following hypotheses were tested: (1) Human iPSC-MSCs can be successfully modified genetically to have NELL1 overexpression; (2) *NELL1* gene-modification of iPSC-MSCs on RGD-grafted CPC will not have adverse effects on cell attachment and proliferation, compared to iPSC-MSCs without *NELL1* gene-modification; (3) *NELL1* gene-modified iPSC-MSCs on RGD-grafted CPC will have greatly enhanced osteogenic differentiation and bone mineral synthesis, compared to control without *NELL1* modification.

2. Methods and materials

2.1. Fabrication of RGD-grafted CPC

CPC powder consisted of TTCP ($Ca_4(PO_4)_2O$) and DCPA ($CaHPO_4$) at 1:1 molar ratio [28]. TTCP was synthesized by heating an equimolar mixture of DCPA and calcium carbonate ($CaCO_3$) (J.T. Baker, Philipsburg, NJ) at 1500 °C for 6 hours (h). TTCP and DCPA powders were then ground and sieved. The median particle sizes of TTCP and DCPA were 17 μm and 1 μm, respectively. Chitosan lactate (Halosource, Redmond, WA) was modified with covalently conjugated G_4RGDSP oligopeptides (Peptides International, Louisville, KY) using carbodiimide chemistry as described previously [10,29,30]. The weight ratio of chitosan/G_4RGDSP was 1000/12.4. The RGD-immobilized chitosan was mixed in distilled water at 8% mass fraction and used as the CPC liquid. A CPC powder:liquid mass ratio of 2 was used. The mixed paste was placed in molds with a diameter of 12 mm and a thickness of 1.5 mm, incubated in a humidor at 37 °C for 4 h, demolded and immersed in water 37 °C for 1 days (d). The RGD-grafted CPC disks were sterilized using an ethylene oxide sterilizer

(Anprolene AN 74i, Andersen, Haw River, NC) for 12 h, and degassed for 7 d before cell seeding.

2.2. Human iPSC culture and derivation of MSCs

The human iPSC BC1 line was generated and kindly supplied by Dr. Linzhao Cheng of the Johns Hopkins University [31,32]. Human primary mononuclear cells (MNCs) were separated from adult marrow by Ficoll-Paque Plus and CD34+ cells were purified using magnetic-activated cell sorting (MACS) system [10]. Bone marrow CD34+ cells were reprogrammed by a single episomal vector pEB-C5 after cultured with hematopoietic cytokines for 4 d [10,31,32].

The iPSCs were cultured on a feeder layer of mitotically-inactivated murine embryonic fibroblasts (MEF) as previously described [10,26]. To derive MSCs, iPSCs were induced to form embryoid bodies (EBs) in Dulbecco's modified Eagle's medium (DMEM)/F12 (Life Technologies, Grand Island, NY) with 20% KnockOut Serum Replacement (serum-free; Life Technologies), 1% MEM non-essential amino acids solution (Life Technologies), 1 mM L-glutamine (Sigma-Aldrich, St. Louis, MO), and 0.1 mM 2-mercaptoethanol (Sigma-Aldrich) in ultra-low-attachment plates (Corning, Corning, NY) for 10 d [10,27]. Then, the EBs were cultured on 0.1% gelatin-coated plates and MSCs which migrated out of EBs were separated mechanically [10,27]. Flow cytometry analysis demonstrated that MSC surface markers were consistently and highly expressed in the iPSC-MSCs [27,33]. The MSC surface markers CD29, CD44, CD166 and CD73 were expressed to levels greater than 90% in these iPSC-MSCs. Expressions of hematopoietic markers, CD31 and CD34, were less than 0.6% in the iPSC-MSCs, while the hESC pluripotency markers, TRA-1-81 and Oct3/4, were less than 0.2% [27,33]. The iPSC-MSCs were cultured in growth medium consisted of low glucose Dulbecco's modified Eagle's medium (DMEM) (Life Technologies) supplemented with 10% hMSC screened fetal bovine serum (FBS) (Thermo Fisher, Logan, UT) and 1% penicillin/streptomycin/glutamine (Life Technologies).

2.3. Lentiviral transduction of iPSC-MSCs

Lentiviruses with *red fluorescent protein* (*RFP*) or human *NELL1* gene driven by EF-1α promoter (GenTarget, San Diego, CA) were used for gene transduction, as previously described [10]. A third generation of human immunodeficiency virus 1 (HIV-1)-based expression lentivector was used to produce lentiviruses [34–36]. *NELL1* was tagged with the human influenza hemagglutinin (HA) epitope at the C-terminal region. The HA epitope tag would facilitate the detection of the recombinant NELL1 protein without interfering with the bioactivity or biodistribution of the recombinant protein. Passage 3 iPSC-MSCs were exposed to 25 multiplicity of infection (MOI) of *RFP* or *NELL1* lentiviruses for 3 d. These cells are referred to as RFP-iPSC-MSCs or NELL1-iPSC-MSCs, respectively.

To evaluate the transduction efficiency and stability, passage 4 to 8 RFP-iPSC-MSCs were examined using epifluorescence microscopy (Eclipse TE2000-S, Nikon, Melville, NY). iPSC-MSCs expressing RFP showed a red fluorescence. The transduction efficiency was further quantified by examining the percentage of RFP-positive cells using FACScan analysis (Becton Dickinson Immunocytometry Systems, San Jose, CA).

The present study used RFP-iPSC-MSCs as control for NELL1-iPSC-MSCs. In our preliminary study, the effect of RFP on osteogenic differentiation was investigated. We compared iPSC-MSCs and RFP-iPSC-MSCs cultured in osteogenic medium on tissue culture polystyrene (TCPS) by Alkaline phosphatase (ALP) activity, quantitative real-time reverse transcription polymerase chain reaction (qRT-PCR), and alizarin Red S (ARS) staining assays. The results suggested that RFP had no significant effect on osteogenic differentiation of iPSC-MSCs.

2.4. qRT-PCR measurement of NELL1 gene overexpression

To examine whether *NELL1* gene transduction was successful and stable, *NELL1* gene expression of NELL1-iPSC-MSCs at passages 4 to 8 was analyzed by qRT-PCR (7900HT, Applied Biosystems, Foster City, CA) using the $2^{-\Delta\Delta Ct}$ method, as described previously [30]. RFP-iPSC-MSCs were used as the control cells. Cells were lysed using the TRIzol reagent and total RNA was purified with the PureLink RNA Mini Kit (Life Technologies). The purified RNA was reverse-transcribed using the High Capacity cDNA Reverse Transcription Kit (Life Technologies). Real-time PCRs were performed with TaqMan Fast Universal PCR Master Mix with No AmpErase UNG (Life Technologies). The TaqMan Gene Expression Assays Hs00196243_m1 and Hs99999905_m1 (Life Technologies) were used for *NELL1* and *glyceraldehyde-3-phosphate dehydrogenase* (*GAPDH*), respectively. *GAPDH* was detected as the control gene.

2.5. Western blot analysis

RFP-iPSC-MSCs and NELL1-iPSC-MSCs were cultured in a 6-well TCPS plate (Sigma-Aldrich). Upon 90% confluence, cells were lysed using 100 μL of M-PER Mammalian Protein Extraction Reagent (Thermo Fisher, Rockford, IL) plus 100 μL Novex Tris-Glycine SDS Sample Buffer (2×) (Life Technologies) for 5 minutes (min). Lysates were spun for 10 min at 16,000 rcf and dithiothreitol (DTT, Sigma-Aldrich) was added to the supernatants to reach a final concentration of 10 mM. Proteins were separated on a 9% SDS-PAGE gel and analyzed by Western blot [37]. The blots were incubated with rabbit anti-HA tag monoclonal antibody (clone C29F4, Cell Signaling, Danvers, MA), mouse anti-NELL1 monoclonal antibody (clone 6A8) and mouse anti-β-actin monoclonal antibody (clone AC-74, Sigma-Aldrich). This was followed by incubation with IRDye 700DX conjugated goat anti-rabbit and IRDye 800 conjugated goat anti-mouse antibodies (Rockland Immunochemicals, Gilbertsville, PA) and detection using the Odyssey system (LI-COR Biosciences, Lincoln, NE). Grey value quantification of the Western blot protein bands was performed using the NIH ImageJ software. Relative HA-NELL1 protein levels were normalized against β-actin.

2.6. ALP activity assay

RFP-iPSC-MSCs and NELL1-iPSC-MSCs (passage 6) were cultured on a CytoOne 24-well TCPS plate (USA Scientific, Ocala, FL) in osteogenic medium. Osteogenic medium consisted of low glucose DMEM supplemented with 10% FBS, 1% penicillin/streptomycin/glutamine, 100 nM dexamethasone, 10 mM _-glycerophosphate and 0.05 mM ascorbic acid (Sigma-Aldrich). ALP activity was measured in order to evaluate the effect of *NELL1* gene

transduction on iPSC-MSC osteogenesis [38]. After 7 and 14 d in osteogenic medium, cells were stained to visualize ALP expression using the Leukocyte Alkaline Phosphatase kit (Sigma-Aldrich) according to the manufacturer's instructions. In parallel, cells were lysed in 250 μL of M-PER Mammalian Protein Extraction Reagent (Thermo Fisher Scientific). ALP activity in lysates was quantified using a LabAssay ALP kit (Wako Pure Chemicals, Osaka, Japan) on a SpectraMax M5 microplate reader (Molecular Devices, Sunnyvale, CA), as described previously [10]. ALP activity was normalized to DNA concentration for each sample using the Quant-iT PicoGreen dsDNA assay kit (Life Technologies).

2.7. Cell growth on RGD-grafted CPC scaffold

RFP-iPSC-MSCs or NELL1-iPSC-MSCs (passage 6) were diluted in growth medium composed of low glucose DMEM supplemented, 10% hMSC screened FBS and 1% penicillin/streptomycin/glutamine, and 150,000 cells were added to each well of a 24-well plate with one RGD-grafted CPC disk. The constructs were cultured in growth medium. At 3 d, disks with RFP-iPSC-MSCs were examined using epifluorescence microscopy to investigate cell attachment and morphology. For measurement of cell growth, RFP-iPSC-MSCs or NELL1-iPSC-MSCs were cultured on disks for 1, 3, 7, and 14 d. Then the discs were fixed with 4% paraformaldehyde (USB, Cleveland, OH), stained with 4',6-Diamidine-2'-phenylindole dihydrochloride at 2 μg/mL (DAPI, Roche, Germany) in Dulbecco's phosphate-buffered saline (D-PBS, Life Technologies) with 0.1% Triton X-100 (Sigma-Aldrich). The discs were examined via epifluorescence microscopy and the number of cell nuclei was counted [39].

2.8. SEM examination of iPSC-MSCs

A scanning electron microscope (SEM) was used to examine the RFP-iPSC-MSC and NELL1-iPSC-MSC attachment on RGD-grafted CPC. Cells cultured on specimens for 3 d in growth medium were washed with D-PBS, fixed with 2.5 % glutaraldehyde, subjected to dehydration using serial diluted ethanol solutions (30%, 50%, 70%, 80%, 90%, and 100% in sequence), and rinsed with hexamethyldisilazane (HMDS) (Sigma-Aldrich) [40]. After evaporation of HMDS in a hood overnight, samples were subsequently sputter-coated with platinum and examined using SEM (Quanta 200, FEI, Hillsboro, OR).

2.9. Osteogenic differentiation of iPSC-MSCs seeded on CPC scaffold

RFP-iPSC-MSCs or NELL1-iPSC-MSCs (passage 6) were diluted in osteogenic medium and added to each well containing one RGD-grafted CPC disk in 24-well plates (1.5×10^5 cells for each well). The constructs were cultured in osteogenic medium which was changed three times per week. At 1, 7, and 14 d, qRT-PCR assay was used to quantify the osteogenic differentiation of RFP-iPSC-MSCs and NELL1-iPSC-MSCs, as described in section 2.4. Taqman Gene Expression Assays (Life Technologies) for *runt-related transcription factor 2* (*RUNX2*) (Assay ID: Hs00231692_m1), *collagen type I alpha 1* (*COL1A1*, Assay ID: Hs00164004_m1), *osteocalcin* (*OC*, Assay ID: Hs00609452_g1), and *GAPDH* (Assay ID: Hs99999905_m1) were used for PCR. RFP-iPSC-MSCs (passage 6) cultured on TCPS in the growth medium for 1 d served as the calibrator [41].

Mineral synthesis by RFP-iPSC-MSCs or NELL1-iPSC-MSCs on TCPS or RGD-grafted CPC was examined by ARS staining. Therefore, After culturing in osteogenic medium for up to 21 d, the samples were fixed using 4% paraformaldehyde and stained with ARS (EMD Millipore, Billerica, MA) for 30 min [42]. The stained deposits were extracted and the ARS concentration was measured using an osteogenesis assay kit (EMD Millipore), following the manufacturer's instructions [42]. RGD-grafted CPC disks without cell seeding were also measured, which were used as a control. The net mineral concentration synthesized by cells was obtained when the control's concentration was subtracted from the concentration of disks with cells.

The cells were typically cultured for up to 14 d according to the previous studies [43,44]. Cell growth, ALP activities, and PCR assays were performed up to 14 days because the values almost reached a peak state after 14 d [43,44]. The mineralization assay was performed at 1, 7, 14, and 21 d, because the previous *in vitro* studies demonstrated that a large amount of calcium content accumulated from 14 d to 21 d during osteogenesis of MSCs [43].

2.10. Statistical analyses

One-way and two-way ANOVA were performed to evaluate the significant effects of the variables. Tukey's multiple comparison tests were used with a p value of 0.05.

3. Results

RFP expression by RFP-iPSC-MSCs at passages of 4 to 8 was examined in order to determine the transduction efficiency and stability of the lentiviral vectors. Representative images are shown in Fig. 1A-D. RFP-iPSC-MSCs stably expressed high levels of RFP from passage 4 to 8. In (E), the percentage of the RFP-positive population was quantified by flow cytometric analysis, showing a transduction efficiency of above 86%. These results indicate that the lentiviral vectors of this study were efficient and stable for gene overexpression.

The *NELL1* expression in the NELL1-iPSC-MSCs was examined by real-time RT-PCR using RFP-iPSC-MSCs as control groups (Fig. 2A). NELL1-iPSC-MSCs at passages of 4 to 8 showed a stable and high level of *NELL1* gene expression, much greater than RFP-iPSC-MSCs ($p < 0.05$). NELL1 overexpression in NELL1-iPSC-MSCs was further confirmed using Western blot analysis. Fig. 2B demonstrated the representative Western blot images of RFP-iPSC-MSCs and NELL1-iPSC-MSCs at passage 6 and 8. Both HA-NELL1 and NELL1 protein levels were consistently higher in NELL1-iPSC-MSCs, irrespective of the passage number. Quantification of HA-NELL1 protein levels showed significant differences between NELL1-iPSC-MSCs and RFP-iPSC-MSCs ($p < 0.05$) (Fig. 2C). These results demonstrate that this study achieved a stable and efficient transduction of *NELL1* in iPSC-MSCs.

RFP-iPSC-MSCs and NELL1-iPSC-MSCs were seeded on TCPS and cultured in osteogenic medium to determine the effect of NELL1 overexpression on iPSC-MSC osteogenesis using ALP activity assay. Fig. 3A-D show representative ALP staining images of RFP-iPSC-MSCs and NELL1-iPSC-MSCs at 7 d and 14 d. ALP staining was more pronounced in

NELL1-iPSC-MSCs than that in RFP-iPSC-MSCs. Quantitative determination of the ALP activity using *p*-nitrophenyl phosphate as the substrate indicated that ALP activity in NELL1-iPSC-MSCs was significantly higher than that in RFP-iPSC-MSCs ($p < 0.05$). ALP activity was increased by 130% at 14 d by NELL1 overexpression. These data demonstrate that NELL1 promoted the osteogenic differentiation of iPSC-MSCs.

RFP-iPSC-MSCs and NELL1-iPSC-MSCs were then seeded on RGD-grafted CPC scaffold. Fluorescent examination showed that RFP-iPSC-MSCs attached, extended, and grew well on RGD-grafted CPC. Fig. 4A showed a representative fluorescent photograph of RFP-iPSC-MSCs at 3 d. Fig. 4B and 4C show SEM micrographs of RFP-iPSC-MSC and NELL1-iPSC-MSC at 3 d which attached and spread well on RGD-grafted CPC. At a higher magnification, long cytoplasmic extensions were indicated by the yellow arrows (Fig. 4D, an example of NELL1-iPSC-MSCs). These observations demonstrated healthy cell function of adhesion and spreading on RGD-grafted CPC. Fig. 4E and 4F show examples of RFP-iPSC-MSC and NELL1-iPSC-MSC nuclei at 14 d. Cell proliferation was evaluated by nuclear counting (Fig. 4G). RFP-iPSC-MSCs and NELL1-iPSC-MSCs expanded on RGD-grafted CPC at a similar rate ($p > 0.05$). Both the RFP-iPSC-MSC and NELL1-iPSC-MSC numbers increased by 2.7-fold from 1 d to 14 d.

In Fig. 5, RFP-iPSC-MSCs and NELL1-iPSC-MSCs on RGD-grafted CPC had increases in *RUNX2*, *COL1A1*, and *OC* expressions. In (A), *RUNX2* expression was higher in NELL1-iPSC-MSCs than in RFP-iPSC-MSCs ($p < 0.05$). At 14 d, *RUNX2* gene level in NELL1-iPSC-MSCs was 2-fold that in RFP-iPSC-MSCs. In (B), NELL1 overexpression increased *COL1A1* at 1 and 7 d ($p < 0.05$). At 7 d, *COL1A1* gene level in NELL1-iPSC-MSCs was 1.7-fold that in RFP-iPSC-MSCs. At 14 d, *COL1A1* gene level in NELL1-iPSC-MSCs and in RFP-iPSC-MSCs was similar ($p > 0.1$). In (C), *OC* was higher in NELL1-iPSC-MSCs than in RFP-iPSC-MSCs ($p < 0.05$). At 14 d, *OC* gene level in NELL1-iPSC-MSCs was 3.1-fold that in RFP-iPSC-MSCs. These results demonstrate that NELL1 overexpression enhanced the osteogenic differentiation of iPSC-MSCs on RGD-grafted CPC.

Mineral synthesis by RFP-iPSC-MSCs and NELL1-iPSC-MSCs on TCPS and RGD-grafted CPC is shown in Fig. 6. At 21 d, the mineralized nodules on TCPS were more pronounced in NELL1-iPSC-MSCs than in RFP-iPSC-MSCs (Fig. 6A and 6B). When cells were seeded on RGD-grafted CPC, ARS staining was deeper and more intense in NELL1-iPSC-MSCs than in RFP-iPSC-MSCs (Fig. 6C-J). Quantitative analysis in Fig. 6K showed that mineral synthesis was enhanced in NELL1-iPSC-MSCs, compared to RFP-iPSC-MSCs ($p < 0.05$). At 14 and 21 d, mineral synthesis by NELL1-iPSC-MSCs was 1.8-fold that by RFP-iPSC-MSCs. These results show that *NELL1* gene modification promoted iPSC-MSC mineralization.

4. Discussion

iPSCs are advantageous for regenerative medicine because they are capable of providing inexhaustible patient-specific stem cells with readily-available cell resources, and avoid ethical controversy and immunologic rejection issues [3,4,45–47]. Moreover, the biosafety for their applications *in vivo* can be improved by deriving MSCs from iPSCs *in vitro* [5].

The present study investigated the effect of *NELL1* gene modified iPSC-MSCs seeded on RGD-grafted CPC for the first time. NELL1 overexpression greatly promoted the osteogenic differentiation and mineral synthesis of iPSC-MSCs on RGD-grafted CPC without significant adverse effect on iPSC-MSC attachment and expansion. Therefore, *NELL1* gene modified iPSC-MSCs combined with RGD-grafted CPC are promising for bone tissue engineering.

The human *NELL1* gene was first identified to be up-regulated in craniosynostosis [48]. NELL1 expression could be increased by certain bone-forming growth factors such as fibroblast growth factor (FGF)-2 and transforming growth factor (TGF)-β1, but not by BMP2 [49]. NELL1 was further found to be able to enhance osteogenic differentiation and mineralization of osteoblasts, BMSCs, and human periodontal ligament stem cells (PDLSCs) [11,49,50]. In addition, NELL1 induced bone regeneration in animal models including rodents and pre-clinical large animals (sheep), and the new bone tissues induced by NELL1 resembled the histological structure of cancellous bone [11,12]. *NELL1* is regulated directly at the transcriptional level by the osteogenic transcription factor RUNX2 which is essential for osteogenic differentiation. NELL1 may function as a key mediator downstream of RUNX2 in control of osteochondrogenesis and, therefore, is highly specific and effective in inducing bone regeneration [12]. One study suggested that NELL1 reduced the transcription of early osteogenic regulators (for example, *ALP*), and induced intermediate and late markers of osteogenic differentiation (for example, *OC*) in osteoblasts [49]. Recently, NELL1 was indicated to increase not only the expressions of late osteogenic markers (*OC* and *COL1*) but also the early osteogenic marker ALP in BMSCs and PDLSCs [50,51]. NELL1 overexpression led to increased *RUNX2* expression in BMSCs [50,51]. In the present study, NELL1 overexpression in iPSC-MSCs significantly up-regulated ALP activity, the expressions of *RUNX2*, *COL1A1*, and *OC*, and the mineral synthesis. These expressions were involved in both the early and the late stages of osteogenic differentiation and were consistent with the findings in BMSCs [51].

Stem cell-based gene therapy has been an important method to effectively enhance tissue engineering efficacy [52]. Delivery of bone-forming growth factors (such as BMPs) by gene transduction can successfully promote bone regeneration [10,11,53]. However, most bone-forming growth factors, including BMPs, are not specific for osteoblasts [53,54]. For *in vivo* usage, superphysiological doses of the growth factors are usually needed in order to induce bone regeneration efficiently. For example, overdose of BMP2 could simultaneously cause potential side effects, such as inflammation, ectopic bone formation, and low quality of regenerated bone tissue with fatty marrow formed inside [11,12,15,55,56]. Therefore, it was necessary to find novel osteogenic growth factors for bone regeneration. NELL1, as a secretory cell factor, works specifically on the osteochondral lineage cells, and hence may have fewer side effects than BMP2 [11,53]. NELL1 cannot induce ectopic bone formation in muscle, which is different form BMP2 [15]. Previous studies compared the effects of *BMP2* and *NELL1* gene overexpression on osteogenic differentiation using goat BMSCs or human adipose-derived stem cells (ADSCs) [11,57]. It was demonstrated that NELL1 and BMP2 had comparable effects on osteogenic differentiation. A recent study genetically modified iPSC-MSCs for overexpressing BMP2, which enhanced the osteogenic differentiation and

bone mineral production [10]. For example, ALP activity was increased by approximately 80% at 14 d and so was bone matrix mineralization at 21 d when BMP2 was overexpressed [10]. In the present study, ALP activity was increased by 130% at 14 d and bone matrix mineralization was increased by 81% at 21 d due to NELL1 overexpression. These results suggest that NELL1 yielded osteogenic differentiation and mineral production of iPSC-MSCs comparable to those of BMP2, consistent with the previous findings [11,57].

Aghaloo *et al.* reported Ad*Nell-1* transduction of BMSCs led to a mixture of both cartilage and bone formation *in vivo* [11]. In the *in vitro* study, they showed NELL1 overexpression enhanced osteogenic differentiation of BMSCs while the effect of NELL1 on chondrogenic differentiation of BMSCs was not detected [11]. A reason is that they cultured MSCs *in vitro* in osteoblastic differentiation media containing ascorbic acid, β-glycerophosphate, and dexamethasone, as we did in the present study. It was the same reason that we did not analyze chondrogenic differentiation of iPSC-MSCs in this study. A recent study demonstrated that recombinant human NELL1 protein delivery enhanced chondrocyte proliferation and cartilaginous extracellular matrix deposition [58]. To our knowledge, there has been no report on whether NELL1 overexpresion would promote chondrogenic differentiation if MSCs are cultured in chondrogenic differentiation media. Further investigation into this interesting issue is needed.

A previous study showed that NELL1 overexpression inhibited the proliferation of goat BMSCs [11]. In another study, however, NELL1 had no inhibition on the proliferation of human ADSCs [57]. In the present study, iPSC-MSCs were seeded on RGD-grafted CPC and the cell growth was determined by nuclear counting. There was no significant difference in cell proliferation between RFP-iPSC-MSCs and NELL1-iPSC-MSCs. Therefore, NELL1 appeared to affect the osteogenic differentiation rather than the proliferation of iPSC-MSCs, consistent with the previous results on ADSCs [57]. RGD was immobilized on chitosan and incorporated into CPC in order to improve cell attachment, growth, and osteogenic differentiation. NELL1-iPSC-MSCs and RFP-iPSC-MSCs attached, extended and grew well on RGD-grafted CPC. Taken together, the novel NELL1-iPSC-MSC and RGD-grafted CPC construct is promising for bone regeneration. Further studies are needed to investigate NELL1-iPSC-MSC seeding of RGD-grafted CPC construct in animal model, and the safety [35] of *NELL1* lentiviral transduction of iPSC-MSCs for bone regeneration *in vivo*.

5. Conclusions

Human iPSC-MSCs were genetically modified for NELL1 protein delivery for the first time, resulting in substantially enhanced osteogenic differentiation while being seeded on RGD-grafted CPC scaffold. Lentiviruses successfully mediated a stable and efficient transduction of *NELL1* in iPSC-MSCs. NELL1 overexpression enhanced osteogenic differentiation and mineral synthesis of iPSC-MSCs on RGD-grafted CPC scaffold, with no significant adverse effects on iPSC-MSC attachment and proliferation. The ALP activity of iPSC-MSCs was increased by 130% at 14 d and the bone matrix mineralization was increased by 81% at 21 d due to NELL1 overexpression. Therefore, human iPSCs are a promising cell source for bone tissue engineering; *NELL1* gene modification of iPSC-MSCs has great potential to enhance

bone regeneration; and RGD-grafted CPC scaffold is suitable for delivering NELL1-iPSC-MSCs for bone regeneration applications.

ACKNOWLEDGMENTS

We thank Prof. Linzhao Cheng of the Johns Hopkins University for providing the iPSCs, and Drs. Michael D. Weir, Jianbo Yang, Laurence C. Chow, Carl G. Simon and Xuedong Zhou for help. This study was supported by NIH NIDCR R01 DE14190 and R21 DE22625 (HX), National Natural Science Foundation of China (NSFC) Grant No. 81030034 (ZZ), the Foundation for the Author of National Excellent Doctoral Dissertation of China Grant No. 201365 (JL), and a bridge fund from the University of Maryland School of Dentistry (HX).

References

1. O'Keefe RJ, Mao J. Bone tissue engineering and regeneration: from discovery to the clinic--an overview. Tissue Eng Part B Rev. 2011; 17:389–392. [PubMed: 21902614]
2. Chen W, Liu J, Manuchehrabadi N, Weir MD, Zhu Z, Xu HH. Umbilical cord and bone marrow mesenchymal stem cell seeding on macroporous calcium phosphate for bone regeneration in rat cranial defects. Biomaterials. 2013; 34:9917–9925. [PubMed: 24054499]
3. Takahashi K, Tanabe K, Ohnuki M, Narita M, Ichisaka T, Tomoda K, et al. Induction of pluripotent stem cells from adult human fibroblasts by defined factors. Cell. 2007; 131:861–872. [PubMed: 18035408]
4. Nelson TJ, Martinez-Fernandez A, Terzic A. Induced pluripotent stem cells: developmental biology to regenerative medicine. Nat Rev Cardiol. 2010; 7:700–710. [PubMed: 20956984]
5. Jung Y, Bauer G, Nolta JA. Concise review: Induced pluripotent stem cell-derived mesenchymal stem cells: progress toward safe clinical products. Stem Cells. 2012; 30:42–47. [PubMed: 21898694]
6. de Peppo GM, Marcos-Campos I, Kahler DJ, Alsalman D, Shang L, Vunjak-Novakovic G, et al. Engineering bone tissue substitutes from human induced pluripotent stem cells. Proc Natl Acad Sci U S A. 2013; 110:8680–8685. [PubMed: 23653480]
7. Teng S, Liu C, Krettek C, Jagodzinski M. The application of induced pluripotent stem cells for bone regeneration: current progress and prospects. Tissue Eng Part B Rev. 2013
8. Villa-Diaz LG, Brown SE, Liu Y, Ross AM, Lahann J, Parent JM, et al. Derivation of mesenchymal stem cells from human induced pluripotent stem cells cultured on synthetic substrates. Stem Cells. 2012; 30:1174–1181. [PubMed: 22415987]
9. Li F, Bronson S, Niyibizi C. Derivation of murine induced pluripotent stem cells (iPS) and assessment of their differentiation toward osteogenic lineage. J Cell Biochem. 2010; 109:643–652. [PubMed: 20039314]
10. Liu J, Chen W, Zhao Z, Xu HH. Reprogramming of mesenchymal stem cells derived from iPSCs seeded on biofunctionalized calcium phosphate scaffold for bone engineering. Biomaterials. 2013; 34:7862–7872. [PubMed: 23891395]
11. Aghaloo T, Jiang X, Soo C, Zhang Z, Zhang X, Hu J, et al. A study of the role of nell-1 gene modified goat bone marrow stromal cells in promoting new bone formation. Mol Ther. 2007; 15:1872–1880. [PubMed: 17653100]
12. Zhang X, Zara J, Siu RK, Ting K, Soo C. The role of NELL-1, a growth factor associated with craniosynostosis, in promoting bone regeneration. J Dent Res. 2010; 89:865–878. [PubMed: 20647499]
13. Li W, Zara JN, Siu RK, Lee M, Aghaloo T, Zhang X, et al. Nell-1 enhances bone regeneration in a rat critical-sized femoral segmental defect model. Plast Reconstr Surg. 2011; 127:580–587. [PubMed: 21285762]
14. Kwak J, Zara JN, Chiang M, Ngo R, Shen J, James AW, et al. NELL-1 injection maintains long-bone quantity and quality in an ovariectomy-induced osteoporotic senile rat model. Tissue Eng Part A. 2013; 19:426–436. [PubMed: 23083222]

15. Cowan CM, Jiang X, Hsu T, Soo C, Zhang B, Wang JZ, et al. Synergistic effects of Nell-1 and BMP-2 on the osteogenic differentiation of myoblasts. J Bone Miner Res. 2007; 22:918–930. [PubMed: 17352654]
16. Ducheyne P, Qiu Q. Bioactive ceramics: the effect of surface reactivity on bone formation and bone cell function. Biomaterials. 1999; 20:2287–2303. [PubMed: 10614935]
17. Pilliar RM, Filiaggi MJ, Wells JD, Grynpas MD, Kandel RA. Porous calcium polyphosphate scaffolds for bone substitute applications -- *in vitro* characterization. Biomaterials. 2001; 22:963–972. [PubMed: 11311015]
18. Deville S, Saiz E, Nalla RK, Tomsia AP. Freezing as a path to build complex composites. Science. 2006; 311:515–518. [PubMed: 16439659]
19. Bohner M, Baroud G. Injectability of calcium phosphate pastes. Biomaterials. 2005; 26:1553–1563. [PubMed: 15522757]
20. Link DP, van den Dolder J, van den Beucken JJ, Wolke JG, Mikos AG, Jansen JA. Bone response and mechanical strength of rabbit femoral defects filled with injectable CaP cements containing TGF-β1 loaded gelatin microparticles. Biomaterials. 2008; 29:675–682. [PubMed: 17996293]
21. Ambrosio L, Guarino V, Sanginario V, Torricelli P, Fini M, Ginebra MP, et al. Injectable calcium-phosphate-based composites for skeletal bone treatments. Biomed Mater. 2012; 7:024113. [PubMed: 22456083]
22. Habib M, Baroud G, Galea L, Bohner M. Evaluation of the ultrasonication process for injectability of hydraulic calcium phosphate pastes. Acta Biomater. 2012; 8:1164–1168. [PubMed: 22075123]
23. Friedman CD, Costantino PD, Takagi S, Chow LC. BoneSource hydroxyapatite cement: a novel biomaterial for craniofacial skeletal tissue engineering and reconstruction. J Biomed Mater Res. 1998; 43:428–432. [PubMed: 9855201]
24. Simon CG Jr, Guthrie WF, Wang FW. Cell seeding into calcium phosphate cement. J Biomed Mater Res A. 2004; 68:628–639. [PubMed: 14986318]
25. Shindo ML, Costantino PD, Friedman CD, Chow LC. Facial skeletal augmentation using hydroxyapatite cement. Arch Otolaryngol Head Neck Surg. 1993; 119:185–190. [PubMed: 8427682]
26. Chen W, Zhou H, Weir MD, Tang M, Bao C, Xu H. Human embryonic stem cell-derived mesenchymal stem cell seeding on calcium phosphate cement-chitosan-RGD scaffold for bone repair. Tissue Eng Part A. 2013; 19:915–927. [PubMed: 23092172]
27. Thein-Han W, Liu J, Xu HH. Induced pluripotent stem cell-derived mesenchymal stem cell seeding on biofunctionalized calcium phosphate cements. Bone Res. 2013; 4:371–384. [PubMed: 24839581]
28. Xu HH, Quinn JB, Takagi S, Chow LC, Eichmiller FC. Strong and macroporous calcium phosphate cement: Effects of porosity and fiber reinforcement on mechanical properties. J Biomed Mater Res. 2001; 57:457–466. [PubMed: 11523041]
29. Park K, Joung Y, Park K, Lee S, Lee M. RGD-Conjugated chitosan-pluronic hydrogels as a cell supported scaffold for articular cartilage regeneration. Macromol Res. 2008; 16:517–523.
30. Liu J, Zhou H, Weir MD, Xu HH, Chen Q, Trotman CA. Fast-degradable microbeads encapsulating human umbilical cord stem cells in alginate for muscle tissue engineering. Tissue Eng Part A. 2012; 18:2303–2314. [PubMed: 22697426]
31. Chou BK, Mali P, Huang X, Ye Z, Dowey SN, Resar LM, et al. Efficient human iPS cell derivation by a non-integrating plasmid from blood cells with unique epigenetic and gene expression signatures. Cell Res. 2011; 21:518–529. [PubMed: 21243013]
32. Cheng L, Hansen NF, Zhao L, Du Y, Zou C, Donovan FX, et al. Low incidence of DNA sequence variation in human induced pluripotent stem cells generated by nonintegrating plasmid expression. Cell Stem Cell. 2012; 10:337–344. [PubMed: 22385660]
33. Tang M, Chen W, Liu J, Weir MD, Cheng L, Xu HHK. Human induced pluripotent stem cell-derived mesenchymal stem cell seeding on calcium phosphate scaffold for bone regeneration. Tissue Eng Part A. 2014; 20:1295–1305. [PubMed: 24279868]
34. Matrai J, Chuah MK, VandenDriessche T. Recent advances in lentiviral vector development and applications. Mol Ther. 2010; 18:477–490. [PubMed: 20087315]

35. Dropulic B. Lentiviral vectors: their molecular design, safety, and use in laboratory and preclinical research. Hum Gene Ther. 2011; 22:649–657. [PubMed: 21486177]
36. Kay MA. State-of-the-art gene-based therapies: the road ahead. Nat Rev Genet. 2011; 12:316–328. [PubMed: 21468099]
37. Bond D, Primrose DA, Foley E. Quantitative evaluation of signaling events in *Drosophila* S2 cells. Biol Proced Online. 2008; 10:20–28. [PubMed: 18385808]
38. Balcerzak M, Hamade E, Zhang L, Pikula S, Azzar G, Radisson J, et al. The roles of annexins and alkaline phosphatase in mineralization process. Acta Biochim Pol. 2003; 50:1019–1038. [PubMed: 14739992]
39. Docheva D, Padula D, Popov C, Weishaupt P, Pragert M, Miosge N, et al. Establishment of immortalized periodontal ligament progenitor cell line and its behavioural analysis on smooth and rough titanium surface. Eur Cell Mater. 2010; 19:228–241. [PubMed: 20473831]
40. Zhao L, Weir MD, Xu HH. Human umbilical cord stem cell encapsulation in calcium phosphate scaffolds for bone engineering. Biomaterials. 2010; 31:3848–3857. [PubMed: 20149437]
41. Liu J, Xu HH, Zhou H, Weir MD, Chen Q, Trotman CA. Human umbilical cord stem cell encapsulation in novel macroporous and injectable fibrin for muscle tissue engineering. Acta Biomater. 2013; 9:4688–4697. [PubMed: 22902812]
42. Zhou H, Weir MD, Xu HH. Effect of cell seeding density on proliferation and osteodifferentiation of umbilical cord stem cells on calcium phosphate cement-fiber scaffold. Tissue Eng Part A. 2011; 17:2603–2613. [PubMed: 21745111]
43. Zhao L, Tang M, Weir MD, Detamore MS, Xu HH. Osteogenic media and rhBMP-2-induced differentiation of umbilical cord mesenchymal stem cells encapsulated in alginate microbeads and integrated in an injectable calcium phosphate-chitosan fibrous scaffold. Tissue Eng Part A. 2011; 17:969–979. [PubMed: 21091340]
44. Zhao L, Weir MD, Xu HH. An injectable calcium phosphate-alginate hydrogel-umbilical cord mesenchymal stem cell paste for bone tissue engineering. Biomaterials. 2010; 31:6502–6510. [PubMed: 20570346]
45. Kaji K, Norrby K, Paca A, Mileikovsky M, Mohseni P, Woltjen K. Virus-free induction of pluripotency and subsequent excision of reprogramming factors. Nature. 2009; 458:771–775. [PubMed: 19252477]
46. Patel M, Yang S. Advances in reprogramming somatic cells to induced pluripotent stem cells. Stem Cell Rev. 2010; 6:367–380. [PubMed: 20336395]
47. Barrilleaux B, Knoepfler PS. Inducing iPSCs to escape the dish. Cell Stem Cell. 2011; 9:103–111. [PubMed: 21816362]
48. Ting K, Vastardis H, Mulliken JB, Soo C, Tieu A, Do H, et al. Human NELL-1 expressed in unilateral coronal synostosis. J Bone Miner Res. 1999; 14:80–89. [PubMed: 9893069]
49. Aghaloo T, Cowan CM, Chou YF, Zhang X, Lee H, Miao S, et al. Nell-1-induced bone regeneration in calvarial defects. Am J Pathol. 2006; 169:903–915. [PubMed: 16936265]
50. Chen CY, Liu YJ, Shi SG, Chen FM, Cai C, Li B, et al. Osteogenic differentiation of human periodontal ligament stem cells expressing lentiviral NEL-like protein 1. Int J Mol Med. 2012; 30:863–869. [PubMed: 22767336]
51. Xia L, Xu Y, Chang Q, Sun X, Zeng D, Zhang W, et al. Maxillary sinus floor elevation using BMP-2 and Nell-1 gene-modified bone marrow stromal cells and TCP in rabbits. Calcif Tissue Int. 2011; 89:53–64. [PubMed: 21584647]
52. Mao JJ, Giannobile WV, Helms JA, Hollister SJ, Krebsbach PH, Longaker MT, et al. Craniofacial tissue engineering by stem cells. J Dent Res. 2006; 85:966–979. [PubMed: 17062735]
53. Xue J, Peng J, Yuan M, Wang A, Zhang L, Liu S, et al. NELL1 promotes high-quality bone regeneration in rat femoral distraction osteogenesis model. Bone. 2011; 48:485–495. [PubMed: 20959151]
54. Ducy P, Karsenty G. The family of bone morphogenetic proteins. Kidney Int. 2000; 57:2207–2214. [PubMed: 10844590]
55. Valentin-Opran A, Wozney J, Csimma C, Lilly L, Riedel GE. Clinical evaluation of recombinant human bone morphogenetic protein-2. Clin Orthop Relat Res. 2002:110–120. [PubMed: 11937870]

56. Shen J, James AW, Zara JN, Asatrian G, Khadarian K, Zhang JB, et al. BMP2-induced inflammation can be suppressed by the osteoinductive growth factor NELL-1. Tissue Eng Part A. 2013; 19:2390–2401. [PubMed: 23758588]

57. Liu Y, Chen C, He H, Wang D, E L, Liu Z, et al. Lentiviral-mediated gene transfer into human adipose-derived stem cells: role of NELL1 versus BMP2 in osteogenesis and adipogenesis *in vitro*. Acta Biochim Biophys Sin (Shanghai). 2012; 44:856–865. [PubMed: 23017834]

58. Lee M, Siu RK, Ting K, Wu BM. Effect of Nell-1 delivery on chondrocyte proliferation and cartilaginous extracellular matrix deposition. Tissue Eng Part A. 2010; 16:1791–1800. [PubMed: 20028218]

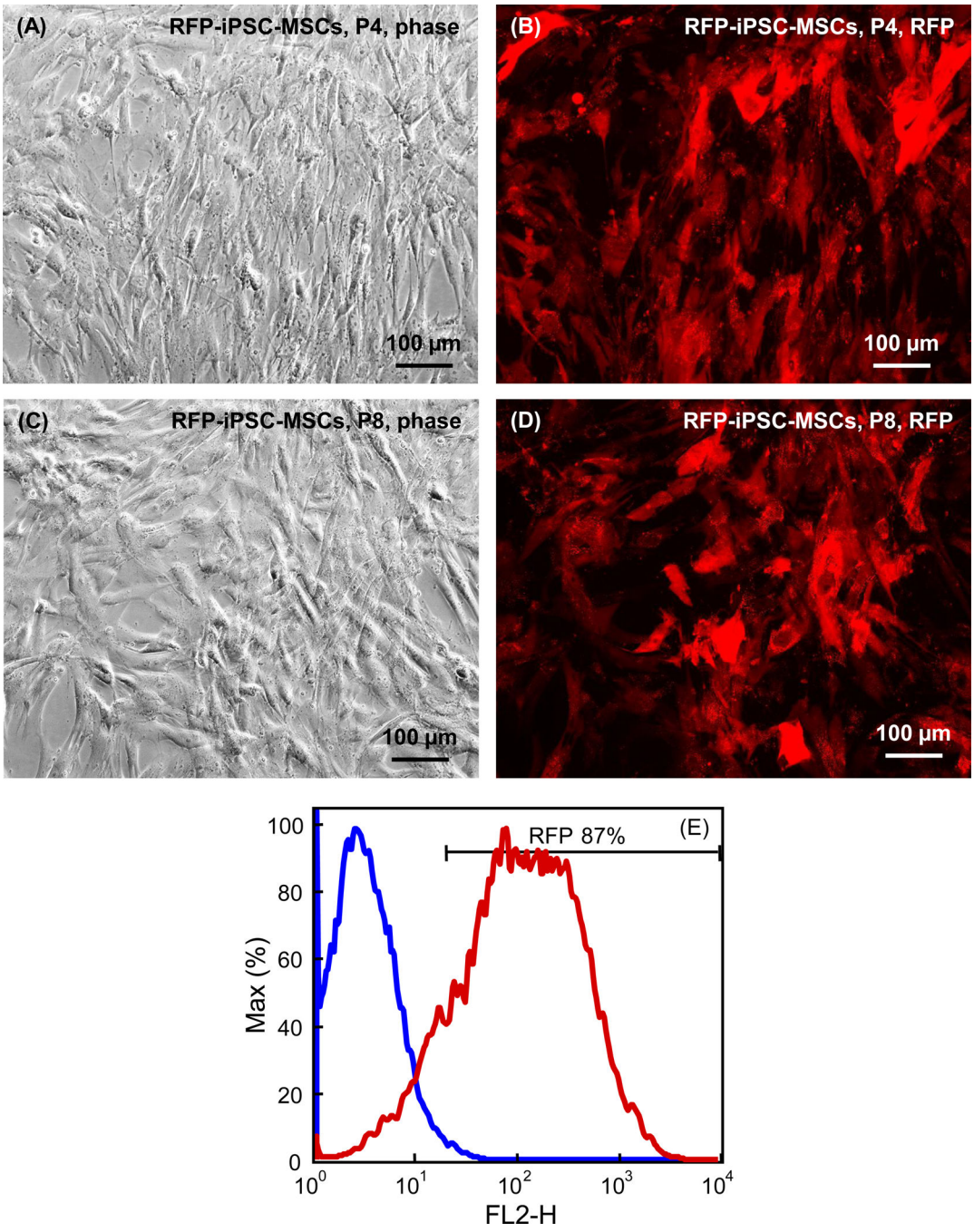

Figure [1].

Red fluorescent protein (RFP) expression in RFP-iPSC-MSCs. (A-D) Representative photographs of RFP-iPSC-MSCs at passages (P) of 4 and 8 taken with a phase-contrast microscope and a fluorescent microscope. In the images, “P” refers to cell passages, “phase” refers to phase-contrast microscopy, and “RFP” refers to fluorescent microscopy. (E) Flow cytometric analysis showing the transduction efficiency of *RFP*-transduced iPSC-MSCs (red line), compared with untransduced iPSC-MSCs (blue line). Representative results from four independent experiments were shown.

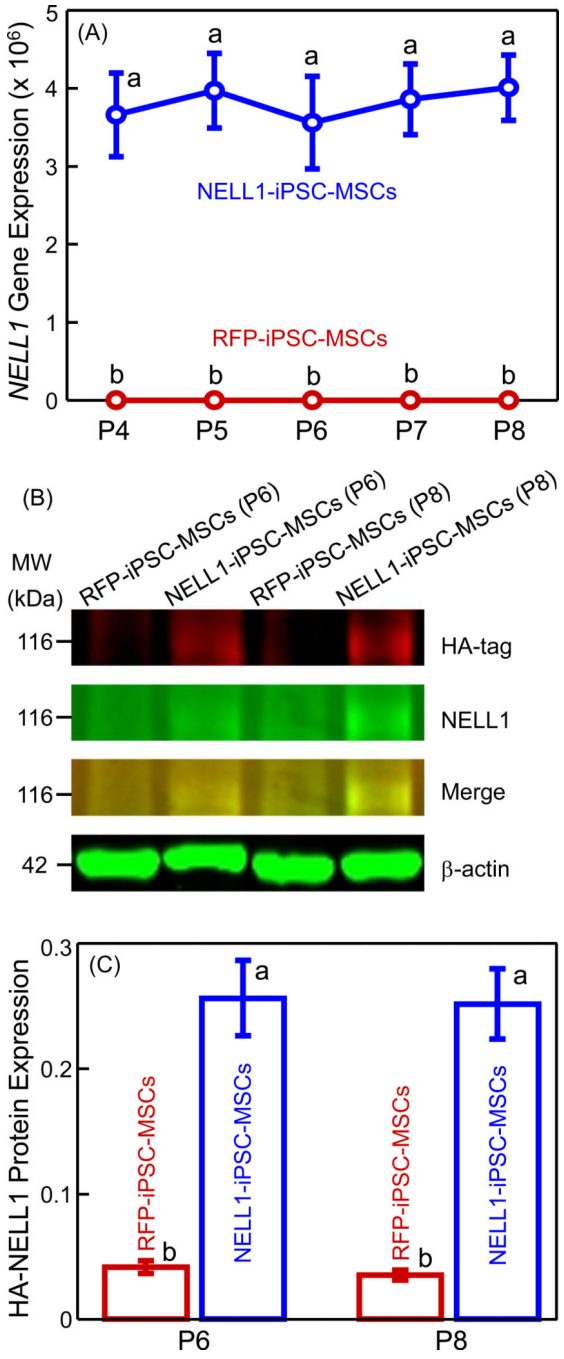

Figure [2].

NELL1 gene and NELL1 protein expression in RFP-iPSC-MSCs and NELL1-iPSC-MSCs. (A) *NELL1* gene expression measured by real-time RT-PCR. (B) Representative images of Western blot analysis of RFP-iPSC-MSCs and NELL1-iPSC-MSCs at passage 6 and 8. (C) Quantitative protein expression of HA-NELL1 determined using Western blot. All data represent the mean ± sd of four independent experiments in (A) and (C). Values indicated by dissimilar letters are significantly different from each other ($p < 0.05$).

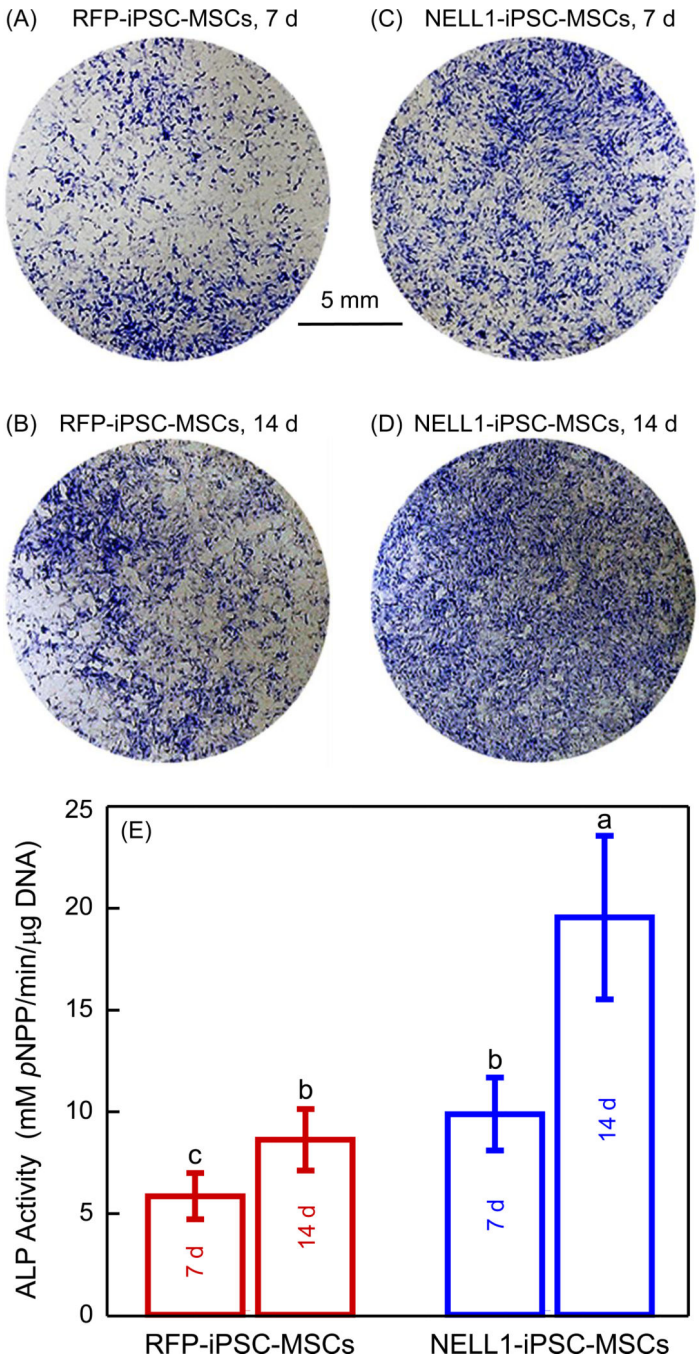

Figure [3].

Alkaline phosphatase (ALP) activity. (A-D) ALP staining of RFP-iPSC-MSCs and NELL1-iPSC-MSCs seeded on tissue culture polystyrene (TCPS) and cultured in osteogenic medium for 7 and 14 d. ALP staining was more pronounced in NELL1-iPSC-MSCs than in RFP-iPSC-MSCs. (E) Quantitative analysis of ALP activity. The results are derived from four separated experiments and expressed as mean ± sd. Values with dissimilar letters are statistically different from each other ($p < 0.05$). ALP activity in NELL1-iPSC-MSCs was significantly higher than that in RFP-iPSC-MSCs.

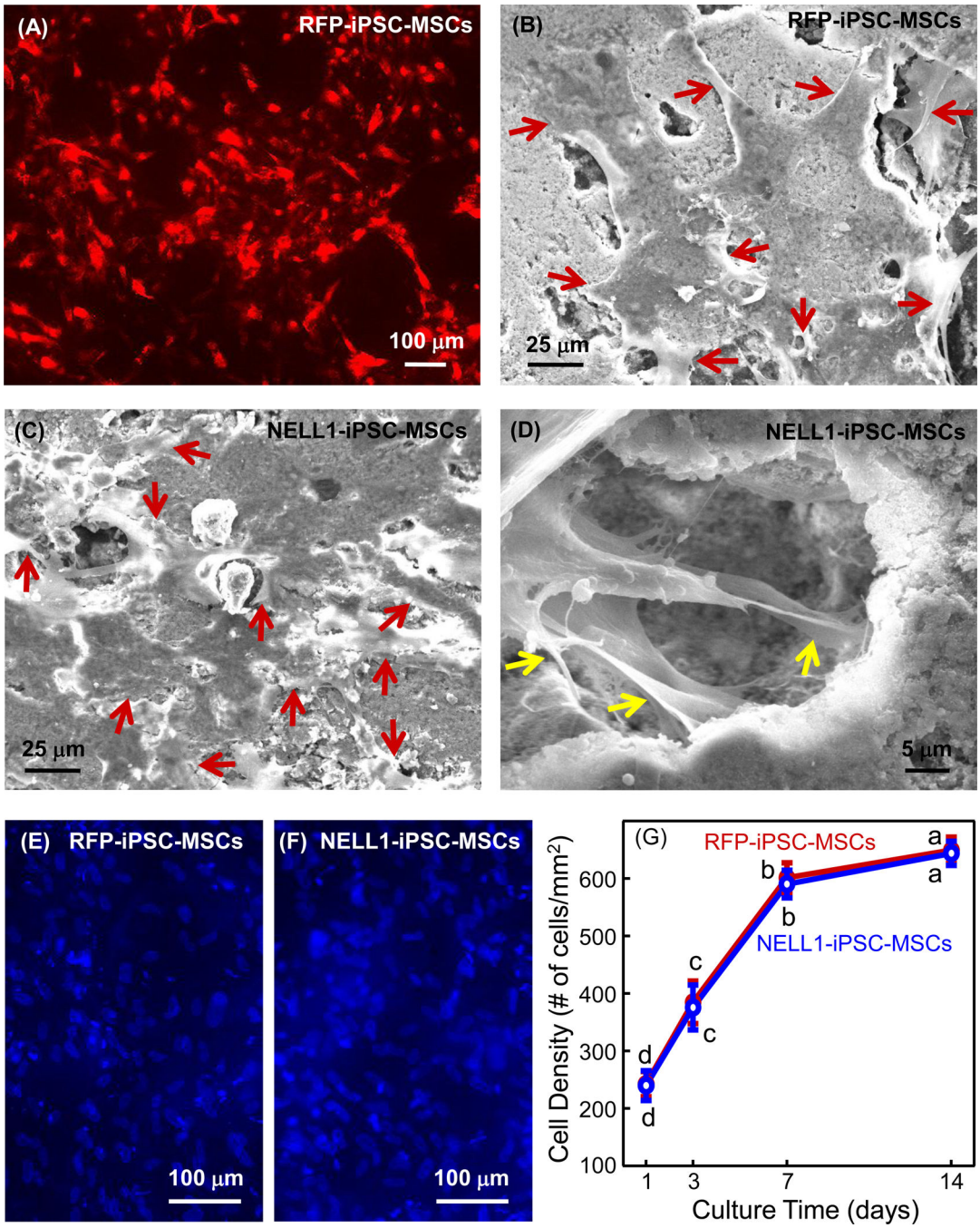

Figure [4].

Analysis of RFP-iPSC-MSC and NELL1-iPSC-MSC growth on RGD-grafted CPC. (A) Fluorescent examination of RFP-iPSC-MSC seeded on RGD-grafted CPC at 3 d. (B-D) SEM evaluation of RFP-iPSC-MSC and NELL1-iPSC-MSC attachment on RGD-grafted CPC at 3 d. The red arrows indicate cells attaching to CPC. Cells spread well and developed long cytoplasmic extensions, which were indicated by yellow arrows in (D) at a higher magnification. (E-G) Determination of cell growth by nuclear counting. The cell nuclei were stained by DAPI. (E) and (F) are typical images at 14 d. Five random fluorescence images

for each sample were analyzed, with four samples, yielding 20 images for each group. In (G), all values are mean ± sd and dissimilar letters indicate significant difference ($p < 0.05$). There was no significant difference between RFP-iPSC-MSCs and NELL1-iPSC-MSCs.

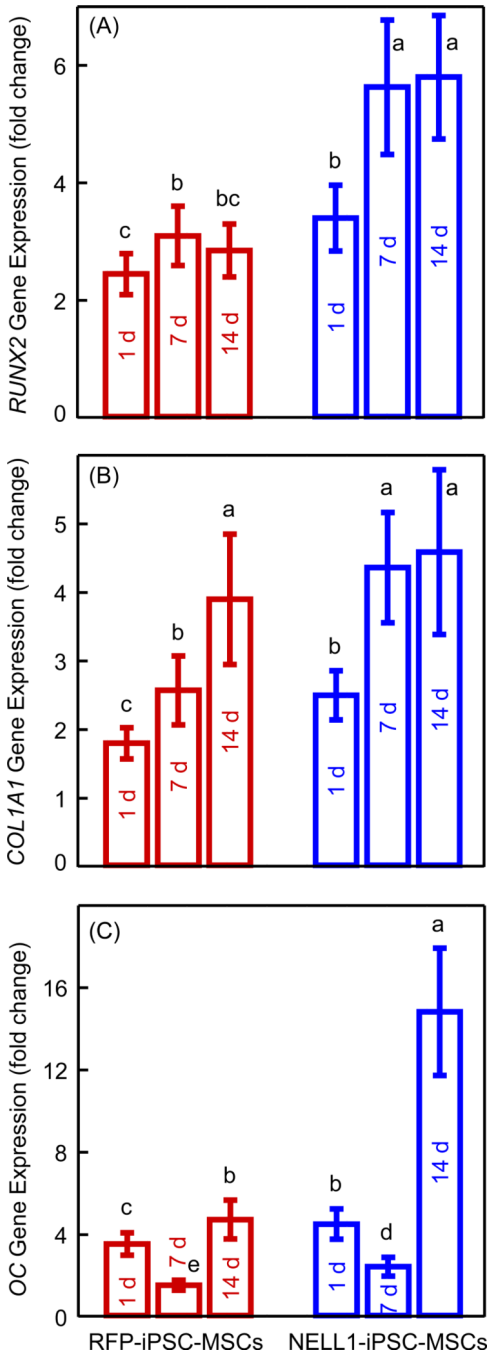

Figure [5].

qRT-PCR assay of osteogenic differentiation of RFP-iPSC-MSCs and NELL1-iPSC-MSCs on RGD-grafted CPC. (A) *RUNX2*, (B) *collagen type 1* (*COL1A1*), and (C) *osteocalcin* (*OC*) gene expressions (mean ± sd; n = 5). Values with dissimilar letters are significantly varied from each other ($p < 0.05$). RFP-iPSC-MSCs and NELL1-iPSC-MSCs underwent osteogenic differentiation with significant increases in *RUNX2*, *COL1A1*, and *OC* expression. *RUNX2* and *OC* were higher in NELL1-iPSC-MSCs than in RFP-iPSC-MSCs at 1, 7, and 14 d.

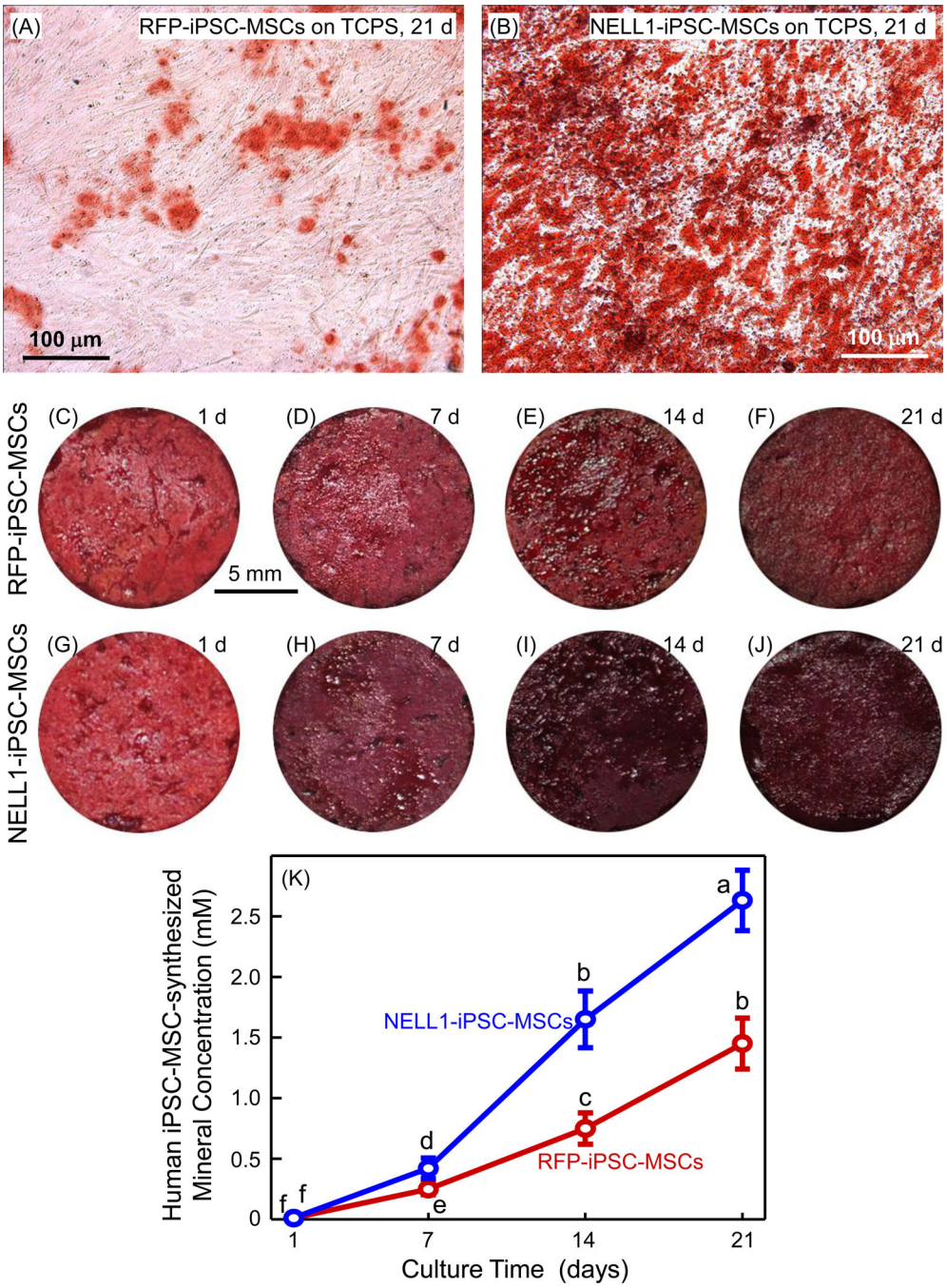

Figure [6].

RFP-iPSC-MSC and NELL1-iPSC-MSC mineral synthesis. (A and B) Cells were seeded on TCPS and examined at 21 d. Calcium deposits were stained red. Mineral nodules were more pronounced in NELL1-iPSC-MSCs than RFP-iPSC-MSCs. (C-K) Cells were seeded on RGD-grafted CPC. ARS staining was performed (C-J) and the results were quantitatively analyzed (mean ± sd; n = 5). (K) ARS staining were deeper and more intense in NELL1-

iPSC-MSCs than in RFP-iPSC-MSCs. Mineral synthesis was enhanced by NELL1 overexpression. Dissimilar letters indicate significant differences ($p < 0.05$).